Imaging of Chronic and Exotic Sinonasal Disease: Review

Arash K. Momeni[1], Catherine C. Roberts[2], and Felix S. Chew[3]

Objective

Chronic sinusitis is one of the most commonly diagnosed illnesses in the United States. The educational objectives of this review article are for the participant to exercise, self-assess, and improve his or her understanding of the imaging evaluation of sinonasal disease.

Conclusion

This article describes the anatomy, pathophysiology, microbiology, and diagnosis of sinonasal disease, including chronic and fungal sinusitis, juvenile nasopharyngeal angiofibroma, inverted papilloma, and chondrosarcoma.

Introduction

Chronic sinusitis is one of the most commonly diagnosed illnesses in the United States. It is estimated to affect more than 30 million individuals and is increasing in incidence [1]. The number of office visits and the annual expenditures on prescription medications for sinusitis rose from $50 million to $200 million from 1989 to 1992 alone. In addition to the economic impact, chronic sinusitis has a significant impact on quality of life. It can lead to significant physical and functional impairment even when compared with chronic debilitating diseases such as congestive heart failure and chronic obstructive pulmonary disease [2].

Sinusitis may be defined as an inflammatory process involving the mucous membranes of the paranasal sinuses or the underlying bone. It is subdivided into acute, subacute, and chronic on the basis of the duration of symptoms [2]. Acute sinusitis is sudden in onset and may last up to 4 weeks. Subacute is a continuum of the natural progression of acute sinusitis and lasts 4–12 weeks. Chronic disease is defined as inflammation of the mucosa of the paranasal sinuses and lasts for at least 12 consecutive weeks [2].

This review focuses on the anatomy, pathophysiology, microbiology, and diagnosis of sinonasal disease, including chronic and fungal sinusitis, juvenile nasopharyngeal angiofibroma, inverted papilloma, and chondrosarcoma.

Anatomy and Pathophysiology

Understanding the normal anatomy and physiology of the paranasal sinuses is important to understanding the pathogenesis of sinus disease. There are four pairs of sinuses named for the bones of the skull they pneumatize. They are the maxillary, ethmoid, frontal, and sphenoid sinus air cells and they are lined by pseudostratified columnar epithelium-bearing cilia. The mucosa contains goblet cells that secrete mucus, which aids in trapping inhaled particles and debris.

The maxillary antrum consists of a roof, floor, and three walls: the medial, anterior, and posterolateral. The roof and medial walls are shared with the orbit and nasal cavity, forming the orbital floor and lateral wall of the nose, respectively [3]. The cilia in the maxillary antrum propel the mucous stream in a starlike pattern from the floor toward the ostium, which is situated superomedially. From the ostium, mucus is swept superiorly through the infundibulum, which is located lateral to the uncinate process and medial to the inferomedial border of the orbit (Figs. 1 and 2). The uncinate process is a sickle-shaped bone extension of the medial maxillary wall that extends anterosuperiorly to posteroinferiorly [4]. The uncinate process is rarely pneumatized. The hiatus semilunaris, situated immediately superior to the uncinate process, is a slitlike air-filled space anterior and inferior to the largest ethmoid air cell, the ethmoidal bulla. It is clinically significant because disease located here results in obstruction of the ipsilateral maxillary antrum, anterior and middle ethmoid air cells, and frontal sinus, whereas disease in the infundibulum results in isolated obstruction of the ipsilateral maxillary sinus alone [5].

Keywords: chondrosarcoma, chronic sinusitis, CT, fungal sinusitis, inverted papilloma, juvenile nasopharyngeal angiofibroma, MRI

DOI:10.2214/AJR.07.7031

Received August 3, 2007; accepted after revision August 29, 2007.

The opinions and assertions contained herein are the private views of the authors and are not to be construed as official or as reflecting the views of the Department of the Air Force or the Department of Defense.

[1]Department of Radiology, David Grant Medical Center, Travis Air Force Base, Fairfield, CA.

[2]Department of Radiology, Mayo Clinic College of Medicine, 5777 E Mayo Blvd., Phoenix, AZ 85054. Address correspondence to C. C. Roberts (roberts.catherine@mayo.edu).

[3]Department of Radiology, University of Washington, Seattle, WA.

AJR 2007;189:S35–S45 0361–803X/07/1886–S35

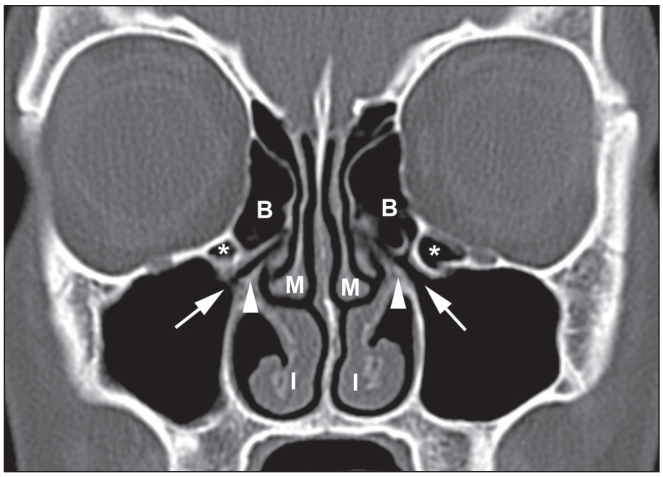

Fig. 1—39-year-old woman with headache. Coronal unenhanced CT scan shows normal sinus anatomy, including each maxillary ostium (*arrows*), uncinate process (*arrowheads*), ethmoid bulla (B), middle nasal turbinate (M), inferior nasal turbinate (I), and infraorbital ethmoid cells or Haller cells (*asterisks*). Maxillary ostium enters infundibulum, which is space between uncinate process and ethmoid bulla.

The entire complex of the maxillary ostium, infundibulum, uncinate process, hiatus semilunaris, ethmoid bulla, and middle meatus make up the ostiomeatal unit or ostiomeatal complex. The ostiomeatal complex (Fig. 3) acts as the common drainage pathway of the frontal, maxillary, and anterior ethmoid air cells, the patency of which is critical for normal sinus drainage and ventilation [4].

Obstruction of the ostiomeatal complex is commonly considered the underlying cause of most cases of sinusitis because obstruction may result in maxillary, ethmoidal, or frontal disease. Predisposing factors that induce local inflammation of the sinonasal mucosa and occlude the ostiomeatal complex include allergy, viral infections, and air pollutants [6]. Mucosal swelling impairs mucociliary clearance and results in sinus ostia obstruction. Sinus excretions then pool and thicken, creating a nidus for superinfection.

The ethmoid sinuses are paired, discrete cells that may number 18 or more. They are anatomically divided into anterior, middle, and posterior groups according to the location of the draining ostia. There are two primary types of cells: intramural and extramural. The intramural cells remain confined to the ethmoid bone, whereas the extramural invade the adjacent bones of the cranial vault or the face [3]. The ethmoid bulla is the air cell directly superior and posterior to the infundibulum and hiatus semilunaris. A large ethmoidal bulla can obstruct the infundibulum and hiatus semilunaris, leading to interference with the drainage of the maxillary and anterior ethmoid sinuses through the ostiomeatal complex [4].

The frontal sinuses drain inferomedially via the frontal recess, which is a space between the inferomedial frontal sinus and the anterior part of the middle meatus. The frontal sinus and the anterior ethmoid air cells together drain directly into the middle meatus via the frontal recess, or less commonly, into the superior ethmoidal infundibulum, before draining to the middle meatus [4].

The sphenoid sinuses drain into the sphenoethmoidal recess, which lies above the superior nasal concha, and the posterior ethmoid cells. Pneumatization of the sphenoid sinuses is slow, but is usually complete by puberty. Still, failure of pneumatization, resulting in a permanent infantile appearance, is not uncommon [3]. The sphenoid sinus is usually septate, but the septum is midline in only 25% of patients [7].

Microbiology

Unlike in acute sinus disease, the exact role of bacteria or other organisms in the cause of chronic sinusitis remains unidentified [8]. Acute illness is classically caused by *Hae-*

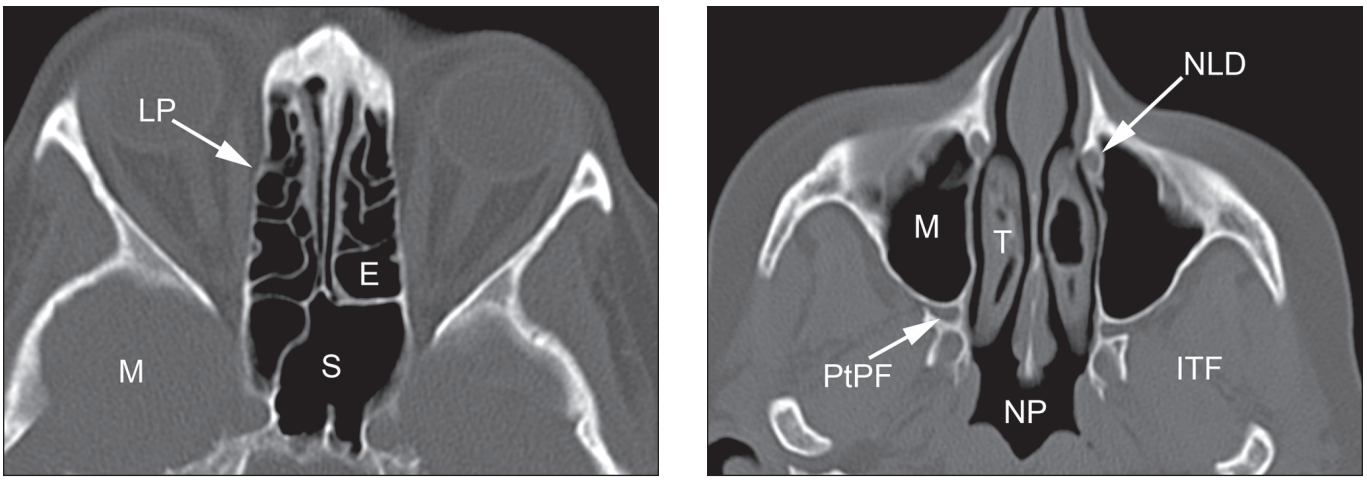

Fig. 2—59-year-old woman with headache.
A and **B,** Noncontiguous axial unenhanced CT images show normal paranasal sinus anatomy. At level of mid globe, ethmoid (E) and sphenoid (S) sinus are visible, as well as middle crania fossa (M) and lamina papyracea (LP). At level of mid face, maxillary (M) sinuses have adjacent nasolacrimal duct (NLD), turbinates (T), pterygopalatine fossa (PtPF), infratemporal fossa (ITF), and nasopharynx (NP).

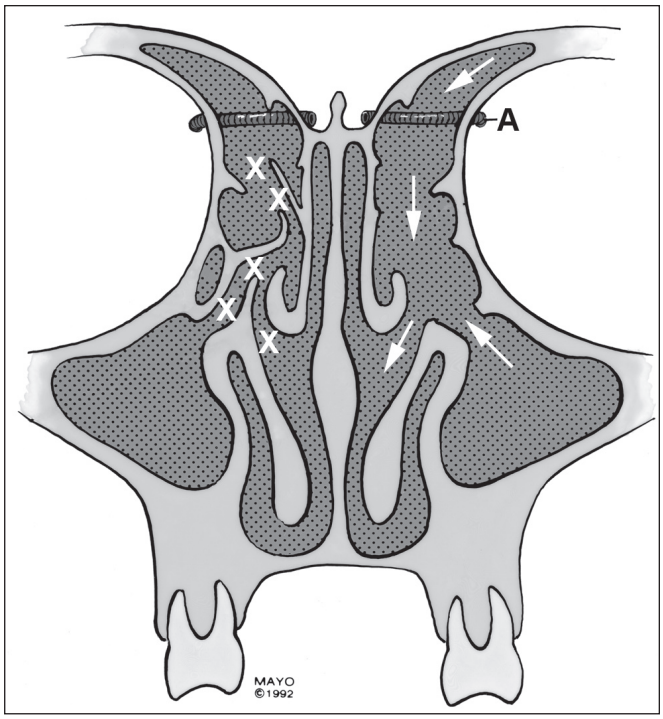

Fig. 3—Anterior drawing of ostiomeatal complex. Arrows show direction of mucociliary clearance. Potential areas of obstruction are denoted with X. Location of anterior ethmoid artery (A) is important in endoscopic sinus surgery. Graphic modified with permission from Mayo Foundation for Education and Research.

mophilus or *Streptococcus* species; however, chronic disease may result from a number of disparate organisms. In a study of 94 cases of endoscopically guided ethmoid sinus cultures from 50 adults with chronic sinusitis, the recovered organisms included *Staphylococcus aureus*, gram-negative rods, *Haemophilus influenzae*, group A streptococci, *Streptococcus pneumoniae*, and *Corynebacterium diphtheriae* [9]. Moreover, polymicrobial infections are more common in patients with chronic sinusitis. The offending organisms of polymicrobial disease include anaerobic bacteria, fungi, and *Pseudomonas aeruginosa* [10].

Chronic Sinusitis

Chronic sinusitis often develops secondary to acute disease that is refractory to treatment. Clinically, few signs or symptoms reliably differentiate acute from chronic disease because they present in a similar fashion. The real distinction is based on the duration of symptoms: acute disease is sudden in onset and may last up to 4 weeks, whereas chronic disease lasts for at least 12 consecutive weeks. The most common presenting symptoms for acute sinusitis include fever and toxicity; chronic sinusitis symptoms include facial pressure, headache, nasal obstruction, postnasal drip, and fatigue.

The location of the facial pain and pressure may also help localize the infection to a particular sinus. Maxillary disease typically causes cheek discomfort or pain in the upper teeth, whereas pain due to frontal sinusitis is usually experienced in the forehead. Ethmoiditis may present with tenderness over the medial canthal region; pain from sphenoid sinus involvement is often retroorbital, but may radiate to the occipital and vertex regions [11].

The two primary diagnostic imaging techniques for evaluating the paranasal sinuses are CT and MRI. Radiography was once the most commonly ordered study; however, CT has surpassed radiography in the evaluation process because of its superior anatomic detail and, when a lower mA protocol is used, a radiation dose similar to a standard four-view radiographic series [12, 13]. CT is the imaging study of choice in both adult and pediatric patients [14].

The primary role of CT is to aid in the diagnosis and management of recurrent and chronic disease and to define the anatomy before surgery. CT can differentiate pathologic variations and show anatomic structures that are inaccessible by physical examination or endoscopy. It is the method of choice for defining the complex sinus anatomy because of its 3D high resolution. CT is the technique of choice in the preoperative evaluation of the nose and paranasal sinuses and is the gold standard for delineation of inflammatory sinus disease resulting from obstruction [15]. The use of a bone algorithm provides excellent resolution of the complete ostiomeatal complex and other anatomic factors that play a role in sinusitis. Coronal CT images most closely correlate with the surgical approach [16]. Therefore, it is the preferred study for the surgeon performing functional endoscopic sinus surgery (FESS) because coronal images simulate the appearance of the sinonasal cavity from the perspective of the endoscope [4]. If an MDCT scanner acquiring near isotropic voxels is used, coronal reformatted images from axial scans are as diagnostic as images acquired in the direct coronal plane. In some cases, reformatted images are preferable to direct coronal images because of decreased dental work artifacts, limited patient mobility, and decreased radiation exposure [17].

The characteristic findings of sinus disease include air–fluid levels, mucosal thickening, and opacification of the normally aerated sinus lumen. The single distinguishing feature of acute sinusitis is the air–fluid level as an isolated finding, whereas the only characteristic finding in chronic sinusitis is sclerotic, thickened bone of the sinus wall [18] (Fig. 4). Mucosal thickening is common to both acute and chronic sinusitis. The differential diagnosis of sinus wall thickening includes fungal sinusitis (mycetoma), which often coexists with chronic sinusitis.

According to Sonkens et al. [19], there are five patterns of inflammatory paranasal sinus disease: infundibular, ostiomeatal unit, sphenoethmoidal recess, sinonasal polyposis and sporadic (unclassifiable). In the infundibular pattern, disease is limited to the infundibulum and the adjacent maxillary sinus; the frontal and ethmoid sinuses are preserved. Pathophysiologic causes for this pattern are swollen mucosa, polypoid lesions, and Haller cells. Infundibulotomy is the therapeutic method of choice and produces excellent results in most cases. In the ostiomeatal unit pattern,

the middle meatus of the nasal cavity and the adjacent anterior and middle ethmoid cells and the maxillary and frontal sinuses are involved. Pathophysiologic causes for this pattern are swollen mucosa, polypoid lesion, concha bullosa, septal deviation, and nasal tumor. Infundibulotomy, in combination with ethmoid bullectomy, is often required. In the sphenoethmoidal recess pattern, the sphenoid sinus and the ipsilateral posterior ethmoid cells are involved. The level of obstruction is in the sphenoethmoidal recess. In the sinonasal polyposis pattern, polypoid lesions fill the nasal cavity and the sinuses bilaterally. In effect, this is a mixture of infundibular, ostiomeatal unit, and sphenoethmoidal recess patterns. In the sporadic (unclassifiable) pattern, the extent of the disease does not appear to be related to the known mucous drainage patterns, and there may be retention cysts, mucoceles, and postsurgical changes.

The extent of disease, according to one of the patterns above, is of particular interest to the otorhinolaryngologist planning therapeutic intervention. Therefore, it is critical to identify the technique of choice for preoperative screening and evaluation. CT is superior to MRI for the delineation of the fine bone structures of the infundibular complex, orbital lamina, orbital floor, and cribriform lamina [20]. Thus, CT is superior to MRI in planning FESS [21]. With MRI, these bone structures have low signal intensity, making them difficult to completely assess (Fig. 5). However, when evaluating for orbital or intracranial complications of sinus disease or surgical intervention, MRI is superior to CT [20, 22, 23].

In their comparison of CT and MRI in the evaluation of inflammatory paranasal disease, Hahnel et al. [20] concluded that CT is superior to MRI in the preoperative planning of FESS. However, MRI may be used as a primary diagnostic instrument in screening for foci of septic disease before implantation of organs or prostheses, in the diagnosis of complications of sinus infection or FESS, and in patients with dental implants. Moreover, MRI might be used to assess therapeutic success in patients with inflammatory disease, with the advantage of avoiding radiation exposure to patients. Therefore, MRI is an alternative to CT in the evaluation of the paranasal sinuses, with its main limitations being a decreased ability to delineate bone detail and its higher cost [19].

Fungal Sinusitis

Fungal sinusitis encompasses a wide variety of infections, from relatively innocuous to rapidly fatal. It should be considered in any patient with chronic inflammation, particularly when the patient is immunocompromised or has intractable symptoms despite adequate bacterial therapy [24]. The two primary forms of fungal disease with the associated imaging characteristics reviewed here include allergic and invasive fungal sinusitis.

Allergic Fungal Sinusitis

Allergic fungal sinusitis is a benign, noninvasive disease caused by a hypersensitivity reaction to fungi in the sinuses. The immune response is predominantly an IgE-mediated type I hypersensitivity reaction; thus, most patients with allergic fungal sinusitis have a history of atopy or asthma. The involved sinuses contain brown or greenish-black material with the consistency of peanut butter or cottage cheese. This material has been called "allergic mucin" and contains laminated accumulations of intact and degenerating eosinophils, Charcot-Leyden crystals, cellular debris, and sparse hyphae rarely visualized without fungal stains. Obstruction of the sinuses, usually due to local lesions such as nasal polyps, a deviated septum, or inflamed mucosa from chronic sinusitis, is required to provide an environment conducive for fungal growth [24].

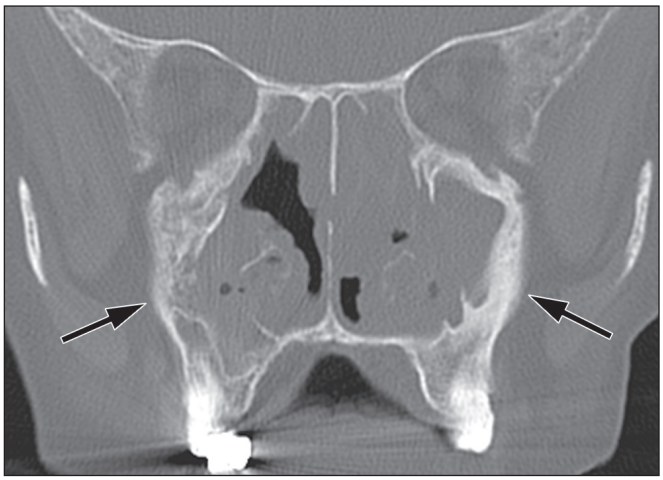

Fig. 4—80-year-old woman with chronic sinusitis. Unenhanced coronal CT scan shows extensive chronic thickening and sclerosis of maxillary sinus walls (*arrows*) and mucosal thickening causing near-complete opacification of sinuses. Intrasinus anatomy is distorted from prior bilateral antrostomies and ethmoidectomies.

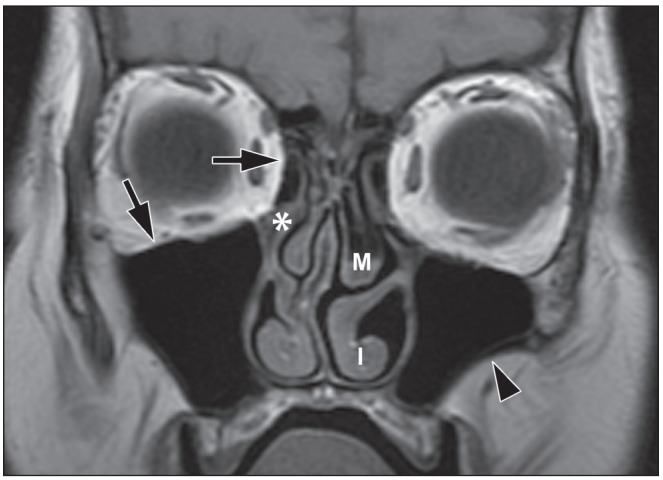

Fig. 5—64-year-old man with history of sinus disease. Coronal T1-weighted MR image shows normal low signal of bone. Orbital lamina and floor (*arrows,* medial and inferior, respectively) and lateral maxillary wall (*arrowhead*) appear as normal low-signal linear structures, accentuated by adjacent high-signal fat. Soft tissue surrounding infundibulum (*asterisk*) is well delineated, as are middle (M) and inferior (I) turbinates.

The most common causative agents of allergic fungal sinusitis are the pigmented fungi, including *Curvularia*, *Bipolaris*, and *Pseudallescheria* species, and the hyaline molds, such as *Aspergillus* and *Fusarium* organisms. Five clinical features aid in the diagnostic evaluation, including radiologically confirmed sinusitis; the presence of mucin in a sinus; visualization of fungal hyphae in the allergic mucin; absence of fungal invasion of the submucosa, blood vessels, or bone; and the absence of diabetes, immunodeficiency disease, or recent treatment with immunosuppressive drugs [24].

Invasive Fungal Sinusitis

Invasive fungal sinusitis primarily occurs in immunosuppressed individuals [23]. The most common causes of immunosuppression in patients with invasive fungal sinusitis include hematologic malignancies, solid organ or bone marrow transplantation, chemotherapy-induced neutropenia, advanced AIDS, or diabetes mellitus [24]. Infection may be attributable to invasion by fungi that have colonized the sinuses or to inhalation of fungal spores. Many patients with invasive fungal sinusitis have a history of chronic sinusitis. Although some have anatomic abnormalities of the sinuses, the anomalies are reported with equal frequency in the asymptomatic population, making it controversial as to whether the anatomic variants predispose patients to fungal colonization [25].

Aspergillus, *Fusarium*, and *Zygomycetes* organisms and pigmented molds are most often implicated in cases of invasive disease [24]. *Aspergillus* species are responsible for acute, fulminant disease with fever, facial pain, nasal congestion, epistaxis, and changes in vision or mentation as common clinical complaints. Diagnosis depends on histopathologic visualization of fungal invasion by biopsy of the involved areas. Although not sufficiently sensitive or specific to confirm diagnosis, imaging techniques such as CT and MRI may show suggestions of fungal sinusitis.

Benign fungal infections secondary to *Aspergillus* species, like allergic fungal sinusitis, are characterized on CT by increased attenuation in the sinuses and frequent bilateral involvement. Complete opacification with expansion, erosion, or remodeling and thinning of the sinuses are characteristic features of allergic fungal sinusitis. However, the signal intensity on T2-weighted sequences is usually low [4]. Intrasinus calcification on CT is also characteristic of fungal sinusitis, particularly that caused by *Aspergillus* species. Calcification may occur with other pathologic processes, such as bacterial sinusitis, mucoceles, and neoplasms, but it is uncommon in nonfungal inflammatory sinonasal disease [26].

Intrasinus calcification on CT with aspergillosis is a characteristic feature of fungal sinusitis and is present in 69–77% of cases [27]. The shape and location of calcification in nonfungal cases are different from those of fungal sinusitis. Calcification in fungal cases is primarily centrally located in the maxillary antrum (Fig. 6), whereas the calcification in nonfungal cases is usually peripheral, near the wall of the maxillary sinus (Fig. 7). Fine punctuate calcification has been identified only in fungal sinusitis, although smooth, marginated, round, or eggshell calcification has been found exclusively with nonfungal disease [28]. Other noteworthy CT features of fungal sinusitis include bone change of a sinus wall (as is seen in chronic sinusitis), a focal mass with increased density in the sinus, and infiltration of adjacent soft tissue or bone destruction in the case of invasive fungal sinusitis. The differential diagnosis of an intrasinus polypoid soft-tissue mass with bone remodeling also includes sinonasal polyposis, sinonasal non-Hodgkin's lymphoma,

Fig. 6—74-year-old man with diabetes and sinus infection caused by *Aspergillus* species. Calcifications (*arrows*) are centrally located in maxillary sinus. Abnormal soft tissue extends through medial wall of maxillary sinus and enters left side of nasal cavity (*arrowheads*).

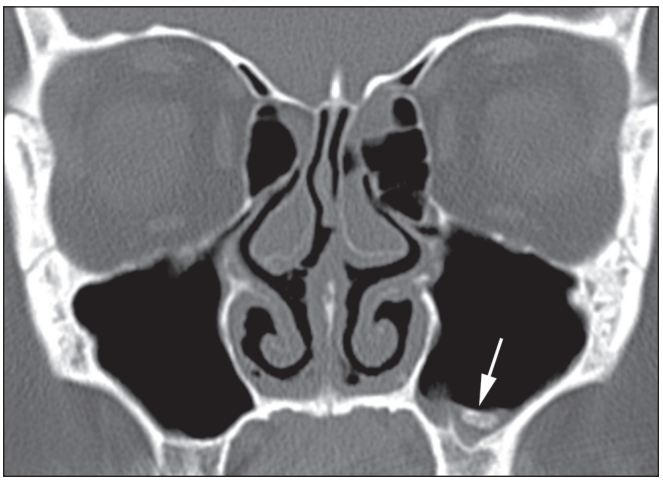

Fig. 7—23-year-old woman with history of multiple episodes of acute sinusitis. Smoothly marginated, peripherally located calcification (*arrow*) is typical of nonfungal disease.

and Wegener's granulomatosis, all of which can be difficult to differentiate with imaging alone.

Invasive fungal infections have a propensity for orbital, cavernous sinus, and neurovascular structure invasion. MRI plays a vital role in the diagnostic evaluation of patients with aggressive fulminant fungal sinus infections by aspergillosis or mucormycosis because of its ability to identify the spread of mycotic infections from the turbinates to the sinuses, orbit, and intracranial cavity [28]. Invasive fungal sinusitis is typically hyperdense on CT and hypointense on

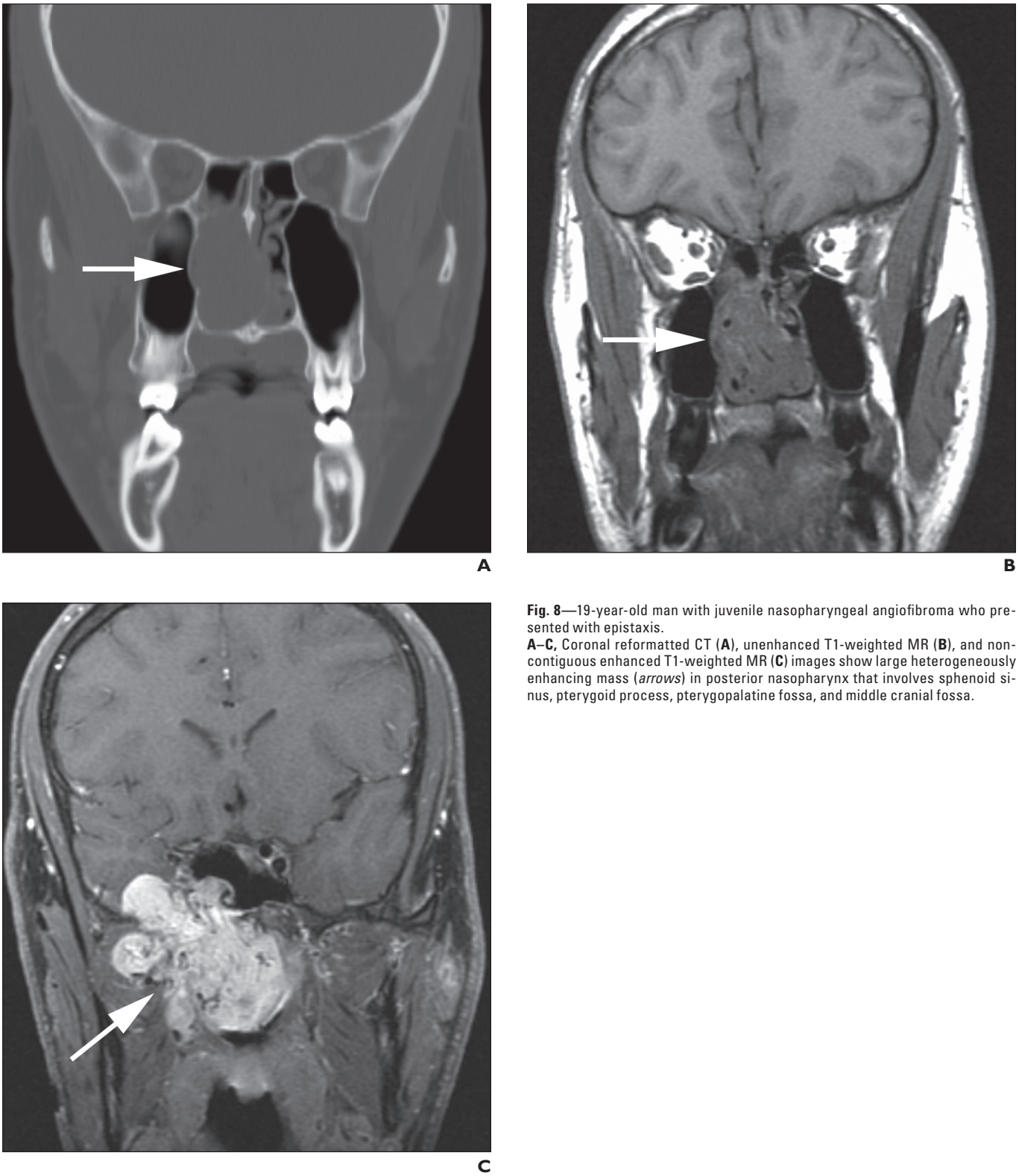

Fig. 8—19-year-old man with juvenile nasopharyngeal angiofibroma who presented with epistaxis.
A–C, Coronal reformatted CT (**A**), unenhanced T1-weighted MR (**B**), and noncontiguous enhanced T1-weighted MR (**C**) images show large heterogeneously enhancing mass (*arrows*) in posterior nasopharynx that involves sphenoid sinus, pterygoid process, pterygopalatine fossa, and middle cranial fossa.

A

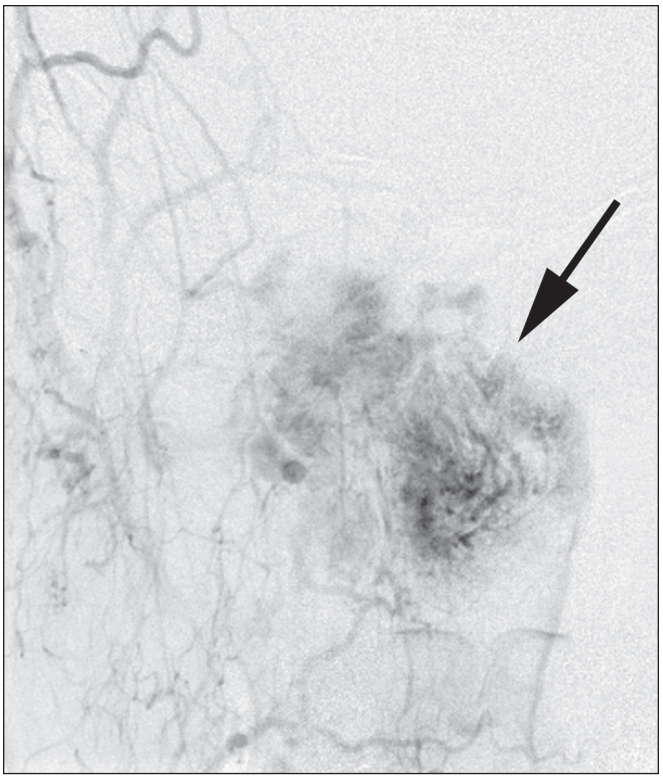

B

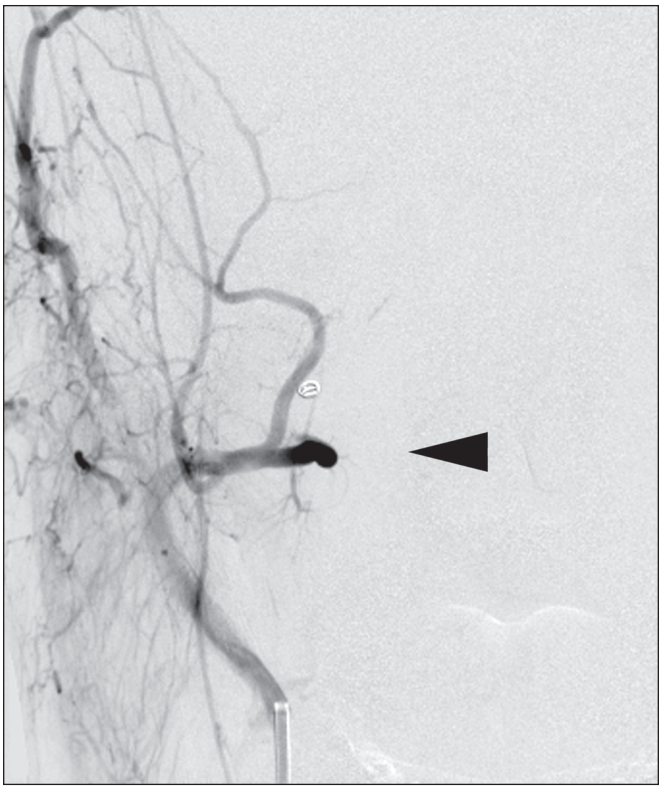

C

Fig. 9—19-year-old man with juvenile nasopharyngeal angiofibroma who presented with epistaxis.
A and **B,** Early (**A**) and late (**B**) anteroposterior arterial phase right internal maxillary artery (IMA) injection angiograms before embolization show marked vascularity of juvenile nasopharyngeal angiofibroma (*arrow*).
C, Early arterial phase right IMA angiogram after embolization shows marked reduction of vascularity (*arrowhead*).

MRI. Immediate detection of this complication can lead to life- or orbit-saving therapy [4].

Juvenile Nasopharyngeal Angiofibroma

Juvenile nasopharyngeal angiofibroma is the most common benign tumor arising from the nasopharynx, but it constitutes only 0.5% of all head and neck neoplasms [29]. These are locally aggressive benign tumors that classically present in adolescent boys with epistaxis. They arise from the fibrovascular stroma of the nasal wall adjacent to the sphenopalatine foramen. The mass characteristically fills the nasopharynx (Fig. 8) and invades the pterygopalatine fossa where it bows the posterior wall of the maxillary sinus anteriorly. Juvenile nasopharyngeal angiofibroma enhances markedly with contrast-enhanced CT, differentiating it from the more rare lymphangioma and from encephaloceles. Other masses that can be found in this location include hypervascular polyps, rhabdomyosarcomas, germ cell tumors, and carcinomas.

The arterial supply of juvenile nasopharyngeal angiofibroma can arise from internal or external carotid artery branches. It is important to have a high clinical suspicion for this lesion because life-threatening hemorrhage may result if a limited resection or biopsy is attempted. Preoperative angiography and embolization (Fig. 9) may reduce surgical blood loss and improve the surgical field of view to facilitate a more complete and uncomplicated surgical resection [5, 30].

Contrast-enhanced CT and MRI are valuable in the evaluation of juvenile nasopharyngeal angiofibroma, with surgical resection being the standard treatment. Despite surgical and imaging enhancements, high recurrence rates have been reported, especially when the juvenile nasopharyngeal angiofibroma involves the skull base. A mean recurrence rate as high as 40–50% in cases of skull base invasion has been reported [31].

Recurrence of juvenile nasopharyngeal angiofibroma is typically due to the growth of residual disease. Early detection of residual disease may allow treatment and recurrence reduction. Kania et al. [31] investigated the diagnostic accuracy of contrast-enhanced CT to detect residual disease immediately after surgical excision of juvenile nasopharyngeal angiofibroma. They state the choice between contrast-enhanced CT and MRI to identify residual disease is open to debate, but they chose CT because it depicts the close interactions between the bone anatomy and residual disease better than MRI and provides good soft-tissue definition.

The results of Kania et al. [31] indicate that contrast-enhanced CT enables early detection of residual disease in the early postoperative stage after lesion excision involving the skull base. The location of residual disease may be correlated with certain extension paths of juvenile nasopharyngeal angiofibroma in the skull base, such as the sphenoid sinus, the base of the pterygoids and clivus, and the cavernous sinus and anterior fossa. To date, most postoperative imaging studies take place between 6 weeks and 6 months after surgery to identify tumors, but not to initiate early management of persistent disease. Because minimally invasive revision surgery may remove the residual disease in most instances, postoperative imaging may be a novel approach in the evaluation process and may help reduce the recurrence rate of juvenile nasopharyngeal angiofibroma.

Inverted Papilloma

Nasal papillomas are uncommon benign neoplasms, accounting for only 0.4–4.7% of all sinonasal tumors [33]. The three most distinct forms are fungiform, cylindric, and inverted papillomas, with inverted papillomas accounting for approximately 47% of all nasal papillomas [32]. Inverted papillomas are benign epithelial neoplasms that classically arise from the lateral nasal wall or maxillary sinus and have significant malignant potential. They most often affect patients 40–70 years old and occur two to four times more often in men than in women. The common symptoms are epistaxis, rhinorrhea, nasal obstruction, anosmia, sinusitis, facial pain, and frontal headache [33]. Proposed staging classification includes stage I, limited to the nasal cavity alone; stage II, limited to the ethmoid sinuses and the medial and superior portions of the maxillary sinuses; stage III, extension to the lateral or inferior aspects of the maxillary sinuses or extension into the frontal or sphenoid sinuses; and stage IV, spread outside the nose and sinuses [4].

Inverted papillomas can be associated with malignancy. Because an increased association with squamous cell carcinoma exists, it is recommended that inverted papillomas be surgically resected with wide mucosal margins. The diagnosis is made by histologic examination of biopsy specimens. Grossly inverted papillomas appear as a mucosal polypoid lesion with histologic changes summarized as patchy severe squamous metaplasia on polypoid protuberances of nasal mucosa and submucosa and in related ductal epithelium. The

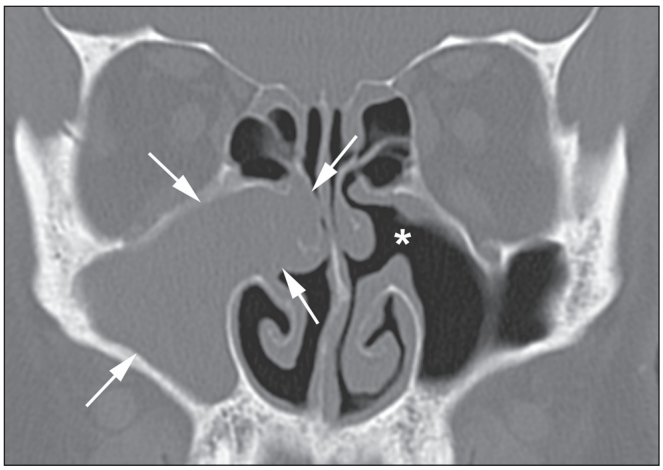

Fig. 10—50-year-old man with intractable nasal congestion. Coronal CT scan of paranasal sinuses shows complete opacification of right maxillary sinus and abnormal soft tissue extending through infundibulum on right into right nasal cavity (*arrows*). CT appearance is nonspecific and could represent polyposis or inverted papilloma. Middle meatal antrostomy has been performed on left (*asterisk*).

polypoid protuberances are possibly formed by invagination of surface mucosa in polyps [34].

Diagnostic imaging may help identify an inverted papilloma when a sinonasal mass with polypoid morphology arises on the lateral nasal wall. CT may show a nonspecific mass centered in the middle meatus with associated bone remodeling (Fig. 10). The diagnosis is evident in only approximately 20% of cases when CT contains stippled calcium. On MRI, the lesion is isodense to muscle on T1-weighted images (Fig. 11A) and isointense to hypointense on T2-weighted images. Most other polypoid masses (sinonasal polyposis, antrochoanal polyp) have high homogeneous signal intensity on T2-weighted sequences. Inverted papillomas enhance (Fig. 11B) and, in roughly 50% of cases, the lesions are heterogeneous in both signal intensity and enhancement. A convoluted cerebriform pattern on T2-weighted sequences or enhanced T1-weighted sequences is typical of inverted papillomas [4, 33]. Juvenile nasopharyngeal angiofibromas tend to be located in the posterior nasal cavity of younger patients. Nasal carcinomas are more likely to destroy bone rather than remodel bone, as is seen with inverted papillomas.

The morphology of a sinonasal mass on MRI in a patient with biopsy-proven inverted papilloma can help warn the surgeon of a probable associated malignancy. Central necrosis in a sinonasal tumor requires consideration of an associated malignancy, even when the preoperative biopsy identifies only an inverted papilloma. Radiologists should be on the lookout for signs of locally invasive disease that might otherwise go unappreciated and greatly alter the surgical approach when a necrotic mass is present. MRI revealing a typical convoluted cerebriform pattern can have small foci of in situ squamous cell carcinoma [33].

Inverted papillomas can show an aggressive pattern of bone destruction because they may cross the cribriform plate into the anterior cranial fossa. They can erode the skull base similar to aggressive cancers and, because signal intensity characteristics overlap those of malignancies, there is no way to preoperatively predict the diagnosis. The lesion is especially problematic for surgeons who treat the condition as if it were malignant by an aggressive surgical approach. Unfortunately, despite aggressive operations, the recurrence rate is 20–40%. Recurrences may be distinguished from postoperative thickening by dy-

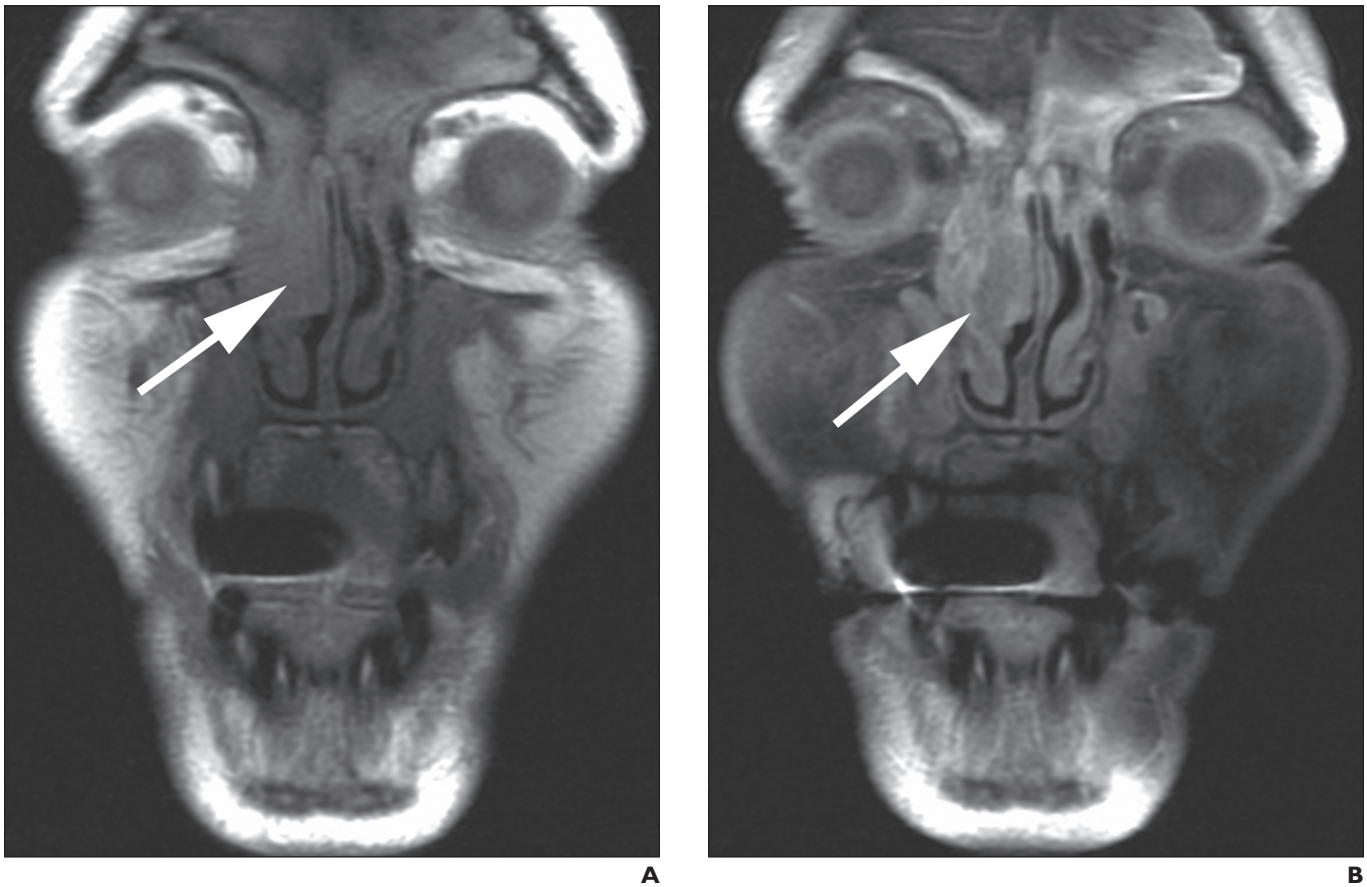

Fig. 11—45-year-old-man with inverted papilloma.
A, Coronal T1-weighted MR image shows mass (*arrow*) in posterior nasopharynx with signal intensity similar to that of muscle.
B, Coronal T1-weighted gadolinium-enhanced MR image highlights mildly enhancing mass (*arrow*), surrounded by more intensely enhancing mucosa.

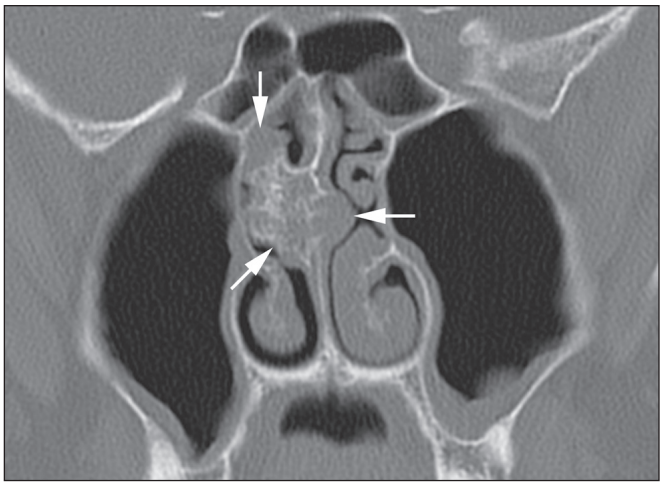

Fig. 12—65-year-old-man with chondrosarcoma of nasal septum. Coronal CT scan of sinuses shows mass with irregular calcification destroying central portion of nasal septum (*arrows*).

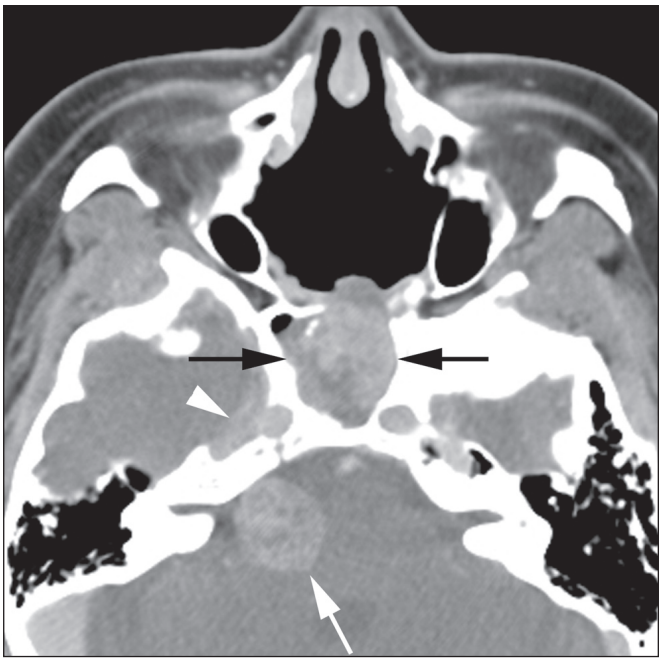

Fig. 13—61-year-old-man with chondrosarcoma of sphenoid sinus. Enhanced axial CT scan shows irregularly enhancing mass in sinus (*black arrows*). Intracranial extension is seen along right cavernous sinus (*arrowhead*) and right cerebellopontine angle (*white arrow*).

namic enhanced MRI; recurrences have earlier and greater enhancement than granulation tissue [4].

Convoluted cerebriform high signal on T2-weighted sequences or enhanced T1-weighted sequences is typical of inverted papillomas [4]. When inverted papilloma is the biopsy result of a sinonasal mass, deviation from the convoluted pattern strongly suggests an alternative diagnosis of concomitant inverted papilloma and squamous cell carcinoma [33].

Chondrosarcoma

Chondrosarcomas are uncommon malignant neoplasms of cartilaginous or osseous origin that account for approximately 11–25% of all primary sarcomatous neoplasms of bone and are most commonly found in the long bones and pelvis. They account for less than 2% of all head and neck tumors, with less than 10% occurring in the craniofacial region [35], making craniofacial chondrosarcoma a rare disease entity.

Craniofacial chondrosarcoma most commonly presents as a painless mass that progresses to symptomatic, with complaints of impaired vision, nasal obstruction, and dental abnormalities. In more rare cases it may also present with swelling of the cheek, headaches, dysphagia, and sensory alterations in the neck, shoulder, and arm. In part because of its rarity, epidemiologic risk factors are poorly defined. The male-to-female ratio is approximately 1.2:1 [36]. Most craniofacial chondrosarcomas occur in patients younger than 40 years and have been reported to develop in association with malignant tumors such as osteosarcoma, melanoma, fibrosarcoma, and leukemia, as well as benign conditions such as Paget's disease and fibrous dysplasia [35].

On CT, craniofacial chondrosarcoma appears as a lobulated mass containing an irregular chondroid matrix with bone invasion and destruction (Fig. 12). The signal density of the chondroid matrix is less than that of the bone matrix, although regions of bone density may be observed because of localized ossification. With T1-weighted sequences, the administration of gadolinium results in curvilinear septal enhancement of the fibrovascular tissues in chondrosarcoma tumors. The unenhanced areas consist mostly of cartilage, mucoid tissue, or necrosis. The chondroid matrix has high signal on T2-weighted sequences because of higher water content, whereas the ossified regions have low signal due to immobile protons [37, 38].

Delineation of chondrosarcoma boundaries relative to normal tissue can be achieved with greater than 98% accuracy using CT and MRI [36]. MRI is the best technique for monitoring tumor recurrence and soft-tissue visualization, thereby allowing differentiation of tumor from surrounding tissues or edema. CT is superior in revealing bone erosion, particularly in the region of the cribriform plate, orbit, pterygopalatine fossae, and infratemporal fossae. Intracranial extension can also be detected as dural enhancement after the administration of contrast material (Fig. 13). Distant metastasis is rare and most often involves the lung; therefore, radionuclide bone scanning plays a limited role in the management of chondrosarcoma [36].

Surgery is the standard of care for patients with chondrosarcoma of the head and neck. Tumors are graded on the basis of cellular activity, nuclear enlargement, and irregularity. Scores of 1, 2, and 3 correspond to low, intermediate, and high grades, respectively. The prognosis is generally good for low- and intermediate-grade chondrosarcoma, with tumor involvement at the resection margin being the only poor prognostic factor other than high-grade disease [36]. The overall 5-year disease-free survival for low-grade chondrosarcoma after complete resection ranges between 54% and 77% [35, 36], with the most common cause of death being recurrence with local skull base invasion [36].

Acknowledgments

We thank Craig Llewellyn at Madigan Army Medical Center, Tacoma, Washington, and Nancy Fischbein at Stanford University, Palo Alto, California, for contributing cases.

References

1. *NIH data book* 1990. Bethesda, MD: US Department of Health and Human Services; 1990, table 44, publication 90-1261
2. Gliklich RE, Metson RN. The health impact of chronic sinusitis in patients seeking otolaryngologic care. *Otolaryngol Head Neck Surg* 1995; 113:104–109
3. Juhl JH, Crummy AB, Kuhlman JE. *Essentials of radiology imaging*, 7th ed. Philadelphia, PA: Lippincott–Raven, 1998:1269–1283
4. Gotwald TF, Zinreich SJ, Corl F, Fishman EK. Three-dimensional volumetric display of the nasal ostiomeatal channels and paranasal sinuses. *AJR* 2001; 176:241–245
5. Brant WE, Helms CA. *Fundamentals of diagnostic radiology*, 2nd ed. Philadelphia, PA: Lippincott Williams & Wilkins, 1999:211–213
6. Yonkers AJ. Sinusitis–inspecting the causes and treatment. *Ear Nose Throat J* 1992; 71:258
7. Goldstein JH, Phillips CD. Current indications and techniques in evaluating inflammatory disease and neoplasia of the sinonasal cavities. *Curr Probl Diagn Radiol* 1998; 27:41–71
8. Bhattacharyya N. The role of infection in chronic rhinosinusitis. *Curr Allergy Asthma Rep* 2002; 2:500–506
9. Doyle PW, Woodham JD. Evaluation of the microbiology of chronic ethmoid sinusitis. *J Clin Microbiol* 1991; 29:2396–2400
10. Shapiro ED, Milmoe GJ, Wald ER, Rodnan JB, Bowen AD. Bacteriology of the maxillary sinuses in patients with cystic fibrosis. *J Infect Dis* 1982; 146:589–593
11. Stafford CT. The clinician's view of sinusitis. *Otolaryngol Head Neck Surg* 1990; 103:870–874
12. Rao VM, el-Noueam KI. Sinonasal imaging: anatomy and pathology. *Radiol Clin North Am* 1998; 36:921–939
13. Tack D, Widelec J, De Maertelaer V, Bailly JM, Delcour C, Gevenois PA. Comparison between low-dose and standard-dose multidetector CT in patients with suspected chronic sinusitis. *AJR* 2003; 181:939–944
14. Kronemer KA, McAlister WH. Sinusitis and its imaging in the pediatric population. *Pediatr Radiol* 1997; 27:837–846
15. Duvoisin B, Landry M, Chapuis L, Krayenbuhl M, Schnyder P. Low-dose CT and inflammatory disease of the paranasal sinuses. *Neuroradiology* 1991; 33:403–406
16. Spector SL, Berstein IL, Li JT, et al. Joint Task Force on Practice Parameters, Joint Council of Allergy, Asthma and Immunology. Parameters for the diagnosis and management of sinusitis. *J Allergy Clin Immunology* 1998, 102(6, part 2): s107–144
17. Takahashi N, Ohkubo M, Higuchi T, Maeda H. Identification of the anterior ethmoid arteries on thin-section axial images and coronal reformatted orbit images by means of multidetector row CT. *Clin Radiol* 2007; 62:376–381
18. Zinreich SJ, Abayram S, Benson ML, Oliverio PJ. The ostiomeatal complex and functional endoscopic surgery. In: Som PM, Curtin HD, eds. *Head and neck imaging*, 4th ed. St. Louis, MO: Mosby, 2003:149–174
19. Sonkens JW, Harnsberger HR, Blanch GM, Babbel RW, Hunt S. The impact of screening sinus CT on the planning of functional endoscopic sinus surgery. *Otolaryngol Head Neck Surg* 1991; 105:802–813
20. Hahnel S, Ertl-Wagner B, Tasman AJ, Forsting M, Jansen O. Relative value of MR imaging as compared with CT in the diagnosis of inflammatory paranasal sinus disease. *Radiology* 1999; 210:171–176
21. Yousem DM. Imaging of sinonasal inflammatory disease. *Radiology* 1993; 188:303–314
22. Eustis HS, Mafee MF, Walton C, Mondonca J. MR imaging and CT of orbital infections and complications in acute rhinosinusitis. *Radiol Clin North Am* 1998; 36:1165–1183
23. Fatterpekar G, Mukherji S, Arbealez A, Maheshwari S, Castillo M. Fungal diseases of the paranasal sinuses. *Semin Ultrasound CT MR* 1999; 20:391–401
24. deShazo RD, Chapin K, Swain RE. Fungal sinusitis. *N Engl J Med* 1997; 337:254–259
25. Jones NS. CT of the paranasal sinuses: a review of the correlation with clinical, surgical and histopathological findings. *Clin Otolaryngol Allied Sci* 2002; 27:11–17
26. Som RM, Lidov M. The significance of sinonasal radiodensities: ossification, calcification, or residual bone? *AJNR* 1994; 15:917–922
27. Yoon JH, Na DG, Byun HS, Koh YH, Chung SK, Dong HJ. Calcification in chronic maxillary sinusitis: comparison of CT findings with histopathologic results. *AJNR* 1999; 20:571–574
28. Larson TL. Sinonasal inflammatory disease: pathophysiology, imaging, and surgery. *Semin Ultrasound CT MR* 1999; 20:379–390
29. Davis KR. Embolization of epistaxis and juvenile nasopharyngeal angiofibromas. *AJR* 1987; 148:209–218
30. Koh E, Frazzini VI, Kagetsu NJ. Epistaxis: vascular anatomy, origins, and endovascular treatment. *AJR* 2000; 174:845–851
31. Kania RE, Sauvaget E, Guichard JP, Chapot R, Huy PT, Herman P. Early postoperative CT scanning for juvenile nasopharyngeal angiofibroma: detection of residual disease. *AJNR* 2005; 26:82–88
32. Som PM, Brandwein MS. Tumors and tumor-like conditions: In: Som PM, Cutin HD, eds. *Head and neck imaging*, 4th ed. St. Louis, MO: Mosby, 2003:261–373
33. Ojiri H, Ujita M, Tada S, Fukuda K. Potentially distinctive features of sinonasal inverted papilloma on MR imaging. *AJR* 2000; 175:465–468
34. Michaels L, Young M. Histogenesis of papillomas of the nose and paranasal sinuses. *Arch Pathol Lab Med* 1995; 119:821–826
35. Koch BB, Karnell LH, Hoffman HT, et al. National cancer database report on chondrosarcoma of the head and neck. *Head Neck* 2000; 22:408–425
36. Ruark DS, Schlehaider UK, Shah JP. Chondrosarcomas of the head and neck. *World J Surg* 1992; 16:1010–1015; discussion 1015–1016
37. Chen CC, Hsu L, Hecht JL, Janecka I. Bimaxillary chondrosarcoma: clinical, radiologic, and histologic correlation. *AJNR* 2002; 23:667–670
38. Geirnaerdt MJ, Bloem JL, Eulderink F, Hogendoorn PC, Taminiau AH. Cartilaginous tumors: correlation of gadolinium–enhanced MR imaging and histopathologic findings. *Radiology* 1993; 186:813–817